Summary of Activities of the Compatibility Working Group in Japan

Hideki Yonezawa
National Traffic Safety and Environment Laboratory
Koji Mizuno
Nagoya University
Takahiro Hirasawa, Hitoshi Kanoshima
Ministry of Land, Infrastructure, Transport and Tourism
Hideaki Ichikawa, Shuji Yamada, Hideki Koga, Akira Yamaguchi
Japan Automobile Manufacture Association
Yuji Arai
Japan Automobile Research Institute
Atsumi Kikuchi
Institute for Traffic Accident Research and Data Analysis

Japan
Paper Number 09-0203

ABSTRACT

In 2006, the Transport Policy Council's Report in Japan stated that it is necessary to discuss compatibility improvement considering the traffic accident environment in Japan. In response to this report, the MLIT has launched the Compatibility Working Group in Japan. This paper summarizes the activities of the WG toward the compatibility improvement.

In the WG, accident analyses and crash tests were performed to identify the safety problem. From global accident data, it is shown that as the front rail of the opposite (or collision partner) car was higher, the injury risk to the occupant tended to be higher. Full frontal car-to-car crash tests were conducted to investigate height matching and mismatching conditions of front rails. It was suggested that matching the front rail heights between two cars provides an overall safety benefit for occupant protection, though the leg injuries may became worse. From the accident analysis and crash tests, it was recognized in the WG that the matching of the front rail heights could be the first issue to be investigated for compatibility improvement.

To evaluate the height of front rails, geometrical measurements and analysis of crash test data can be considered. The footprint of the front rails can be observed in the measured barrier force distribution of a full-width rigid barrier test. Accordingly, to evaluate the front rail heights, measurement and evaluation of the barrier force distribution using high-resolution load cells in a full-width rigid barrier test was investigated. Several methods were developed and proposed for evaluating the front rail heights based on the barrier force distributions.

INTRODUCTION

Transport Policy Council's Report in Japan (June 2006) [1] states in the section of "Enhancement of Passive Safety Measures" that "As another passive safety measure, it will be necessary to formulate a compatibility regulation relating to occupant protection in an accident between vehicles of different sizes in keeping with available research results and the drafting of a similar international regulation." In response to this report, the Ministry of Land, Infrastructure, Transport and Tourism (MLIT) has launched the Compatibility Working Group (WG) in Japan to investigate measures of compatibility.

In vehicle compatibility, it is recognized that good structural interaction is a prerequisite to ensure the efficient energy absorption of frontal structures and the integrity of the passenger compartment. For good structural interaction, matching the heights of front rails above the ground is one of the important factors. In compatibility, the aggressiveness of the sports

utility vehicle (SUV) is one of significant issues to be addressed. In 2003, the Front-to-Front Compatibility Technical Working Group (TWG) of the US Alliance announced Phase I requirements for improving geometrical compatibility [2]. In the Phase I, it was required that either (1) the primary energy absorbing structure (PEAS) shall overlap the FMVSS Part 581 bumper zone (Option 1) or (2) a secondary energy-absorbing structure (SEAS) shall be installed, whose lower edge shall be no higher than the bottom of the Part 518 bumper zone (Option 2).

The MLIT has conducted accident analyses and crash tests. The Japan Compatibility WG examined the results of these analyses. The WG focused on the front rail height matching in car-to-car collisions. In order to evaluate the front rail height, candidate test procedures based on measurement and evaluation of the barrier force distribution in a full-width rigid barrier (FWRB) crash test were proposed in the WG.

ACCIDENT ANALYSIS

The relationship between front rail heights and injury risks to drivers were examined using global and in-depth accident data in Japan.

Global Accident Data Analysis

National accident data (police data) in Japan was used to investigate the compatibility situation. Vehicle-to-vehicle collisions, where both vehicle drivers were belted, were selected for the analysis. Table 1 presents the number of injured drivers in head-on collisions. The number of belted drivers in cars involved in car-to-vehicle head-on collisions in the time span from 2001 to 2007 was 119,692, and the probability of fatal and serious injuries was 7.3%. The number of car-to-car collisions during this time was 91,766. In order to examine late model cars, models tested by the Japan New Car Assessment Program (JNCAP) as of 2002 were selected as the subject cars (N=3,856). Furthermore, among these collisions involving the car models tested by JNCAP, the other collision partner cars were limited to those registered as of 2000, which led to the population of 1,308 collisions. This research focused on these 1,308 collisions.

Figure 1 shows the probability of fatal and serious injuries to belted drivers by the curb mass of the subject car. The probability of injury in the subject car decreases and that in the collision partner car increases with increasing subject car mass. The probability of fatal and serious injury of the drivers in the subject and the collision partner cars are comparable when the subject car mass in the range of 1,100 to 1,300 kg.

Table 1. Number and probability of injuries of drivers in cars in head-on collisions (both drivers were belted in collisions)

Subject car			Number of drivers					Prob. of fatal and serious injury (%)
			Fatal	Serious	Minor	No injury	Total	
Car-to-vehicle collision			1,056	7,667	62,640	48,329	119,692	7.3
Car-to-car collision	Car		309	4,990	48,169	38,298	91,766	5.8
	JNCAP car	Subject	3	187	2,263	1,403	3,856	4.9
		Other	17	202	1,966	1,671	3,856	5.7
	JNCAP car vs. car (registered 2000 or later)	Subject	1	69	753	485	1,308	5.4
		Other	3	62	729	514	1,308	5.0
		Total	4	131	1,482	999	2,616	5.2

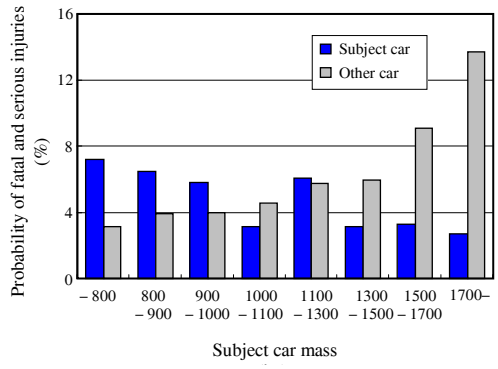

Figure 1. Car curb mass and probability of injuries to belted driver

The number of driver injuries is presented in Table 2 as a function of the front rail ground height of the subject car. The front rail height is defined as the average of ground heights between the upper and lower edges of the front rail front-end. The number of cars with a front rail height ranging from 425 to 475 mm is 1,174, which account for 44.9% in the vehicle fleet. The number of cars with their front rail height ranging from 400 mm or less and from 500 mm or more is 195 and 277, respectively. Front rail heights of many cars in the Japanese car fleet are included in the FMVSS Part 581 bumper zone (i.e., 406 to 508 mm).

Figure 2 shows the probability of injuries to drivers by the front rail height of the subject car. Within the range from 400 to 500 mm of front rail height, the probability of injuries in the subject car tends to decrease with a higher front rail, whereas in the collision partner car the probability tends to increase. However, this tendency is not observed in the ranges where the front rail height is less than 400 mm or when it is greater than 500 mm. One reason may be the number of subject cars is small in these ranges (see Table 2).

Table 2. Front rail height of subject car and the number of belted driver injuries

Front rail height (mm)	Subject car					Other car				
	Fatal	Serious	Minor	No injury	Total	Fatal	Serious	Minor	No injury	Total
– 400		10	117	68	195		10	103	82	195
400 – 425	1	24	196	128	349		9	207	133	349
425 – 450	3	31	291	212	537	2	23	320	192	537
450 – 475		29	361	247	637	2	37	358	240	637
475 – 500		31	361	229	621		38	346	237	621
500 – 525		6	132	95	233		13	124	96	233
525 –			24	20	44		1	24	19	44
Total			1482	999	2616	4	131	1482	999	2616

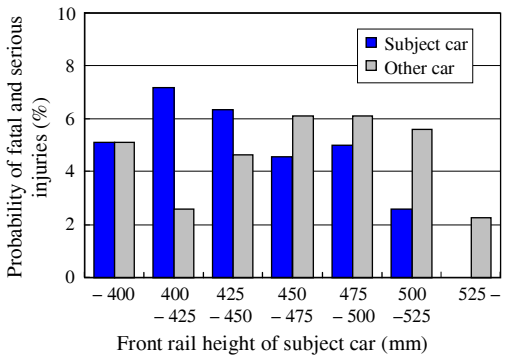

Figure 2. Front rail height of subject car and the probability of belted driver injuries

The injury risks to belted drivers were examined by the relative height (ΔH) of the front rail of the subject car with respect to the collision partner car. When ΔH is positive, the front rail of the subject car is higher than that of the collision partner car; and conversely, when ΔH is negative, the front rail is lower than that of the collision partner.

The number of involved drivers and the probability of fatal and serious injury by relative front rail height ΔH are shown in Figure 3. There is an observable trend that the probability of fatal and serious injury was lower as the relative front rail height ΔH was lower. The probability of serious injury to belted drivers was 7.7% for cars with ΔH of 70 mm or less. In contrast, it was 4.3% for cars with a ΔH of 70 mm or more.

Figure 4 and Figure 5 show the probability of fatal and serious injuries of belted drivers by subject car mass and the relative front rail height ΔH. The collisions were classified into groups in which ΔH ranged from -40 to 40 mm (see Figure 4) and from -25 to 25 mm (see Figure 5). The probability of driver injury of the subject car and the other car is slightly smaller for collisions in which the relative front rail height ΔH was in the range from -40 to 40 mm. However, this trend was opposite, where the injury risk to drivers was higher for the group where the relative front rail height ΔH ranged from -25 to 25 mm.

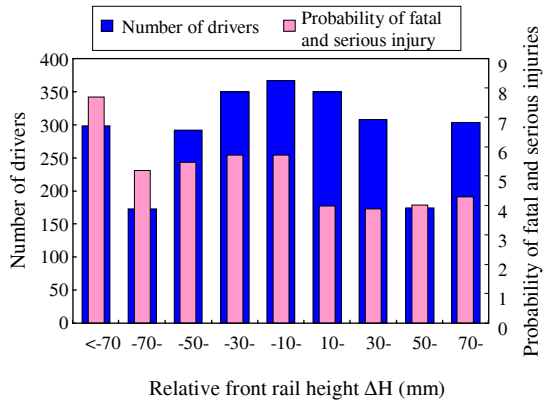

Figure 3. The probability of belted driver injuries by subject car relative front rail height

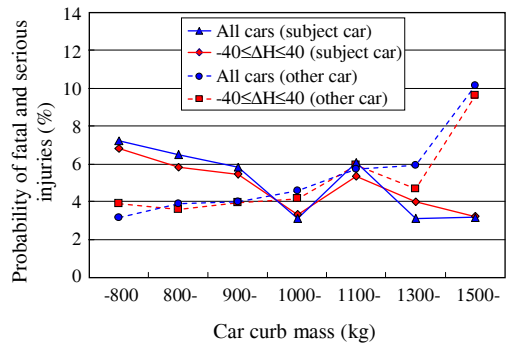

Figure 4. The probability of belted driver injuries by subject car mass and relative front rail height (ΔH) of -40 to 40 mm

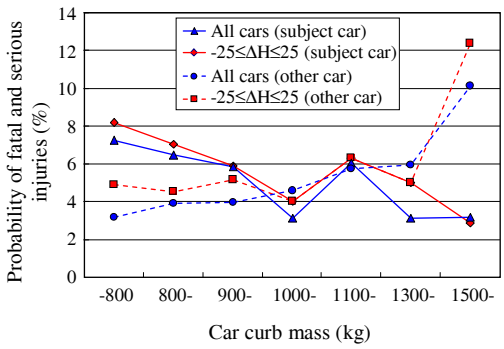

Figure 5. The probability of belted driver injuries by subject car mass and relative front rail height ΔH of -25 to 25 mm

Table 3 presents the probability of fatal and serious injuries to belted drivers classified by subject car types versus the ΔH divided into three ranges—less than 40 mm, -40 to 40 mm, and greater than 40 mm. When the relative front rail height ΔH is in the range from -40 to 40 mm, the injury risks to driver tend to be smaller than for the other two groups.

In accident data, many factors can affect injuries to drivers. The front rail height is one of design factors, which can be associated with vehicle mass, stiffness, and vehicle type. More research on accidents is needed to identify the effectiveness of front rail height matching. The influences of vehicle mass and stiffness also will be investigated in the WG to make clear the problem of compatibility.

Table 3. Probability of fatal and serious injuries to belted drivers in subject cars by relative front rail height differences

Front rail height of subject car from other car	Prob. injury of driver in subject car		
	Minicar	Small car	MPV
ΔH ≤ −40 mm	7.5%	6.5%	5.9%
−40 mm < ΔH < 40 mm	6.3%	4.4%	3.2%
ΔH ≥ 40 mm	9.1%	3.9%	3.9%

In-Depth Accident Data Analysis

From in-depth accident database of Institute for Traffic Accident Research and Data Analysis (ITARDA) from 1994 to 2008, 34 head-on collisions between cars were extracted. The involved vehicles consisted of 62 cars, 5 Multi Purpose Vehicles (MPVs) or SUVs, and one 1-BOX type vehicles. In the data, the cross-section height, upper edge and lower edge ground heights of front rails were distributed 60–170 mm, 378–600 mm, and 256–500 mm, respectively.

Figure 6 shows the relation between override/underride occurrence and the relative front rail height. The override/underride occurrences were identified from photographs of cars in accidents by comparing the crush depth of the upper and the lower structures. Although the override or underride tendency is not clearly defined, it may occur when the front rail height difference is 100 mm or more.

The intrusion into the passenger compartment is shown in Figure 7 by the front rail relative height ΔH and the barrier equivalent velocity (BEV). The compartment intrusion started to initiate at a BEV of 25 km/h, and tended to increase with increasing BEV. The compartment intrusion tended to be small as the front rail difference was close to zero. There were cars with intrusions of 450 mm (ΔH=-140 mm) and 500 mm (ΔH=121 mm) at a BEV of60 km/h, and where the intrusion was related to the survival space in these accidents.

The injury severities of belted drivers are also shown by the Maximum Abbreviated Injury Scale (MAIS) in Figure 8. The MAIS tended to be large as the front rail height difference was large. However, the MAIS also tended to be large as the front rail height difference was small. When the front rail heights of two collided cars matched each other, the car acceleration can be higher than where there is no matching. The acceleration-related injuries such as the restraint system injury might be one of the causes for this tendency.

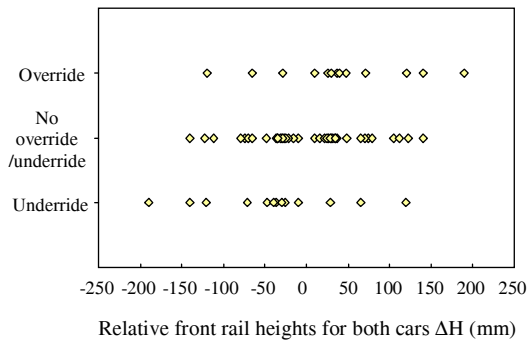

Figure 6. Override/underride based on in-depth accident data

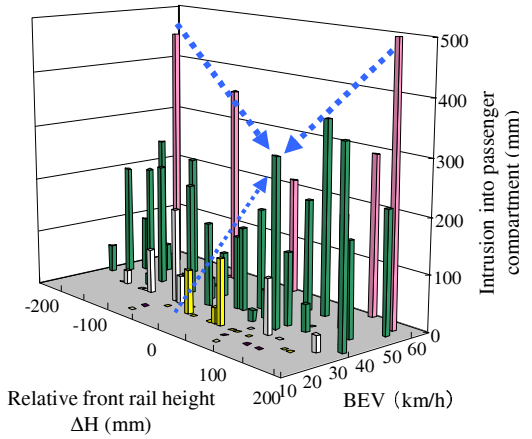

Figure 7. Relation between passenger compartment intrusion, relative front rail height, and barrier equivalent velocity

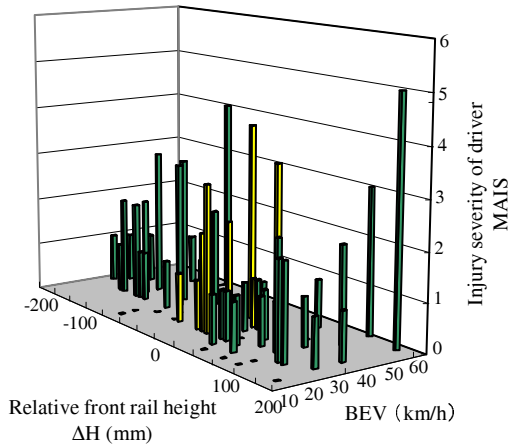

Figure 8. Injury severity of belted driver by front rail ground height and barrier equivalent velocity

CRASH TESTS

Full frontal car-to-car crash tests were conducted for a minicar and a large car, for which the heights of their front rails were different, and for which the ride heights of both cars were adjusted so that the front rail heights were aligned. The car accelerations and dummy responses were examined, and also compared to those in the FWRB test at 55 km/h conducted by JNCAP.

Test Method

A minicar and a large car were impacted center line-to-center line with 100% overlap of the minicar (Figure 9). The velocity of each car at the time of impact was 50 km/. Figure 2 shows the geometry of the front rails of both cars. In Test 1, the front rail of the large car was higher than that of the minicar by 130 mm, as measured at the location of the center of the cross sections across the front rails. Due to the height difference, the front rails of both cars would not contact (or interact with) each other. In Test 2, the ride height of the minicar was raised and that of the large car was lowered so that the geometric centers of the front rails of both cars were aligned. In the lateral direction, the front rails of both cars overlapped each other. In each car, a Hybrid III AM50 dummy was seated in both the driver seat (right) and front passenger seat (left) and was restrained with a seat belt. The test weights of the minicar and the large car were 1024 kg (curb mass 820 kg) and 1695 kg (curb mass 1510 kg), respectively; and the ratio of the large car-to-minicar test mass was 1.6.

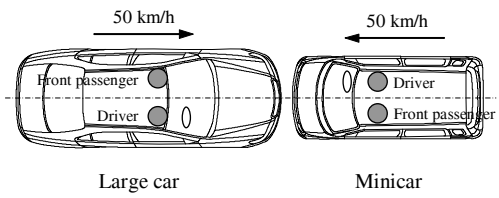

Figure 9. Crash configuration

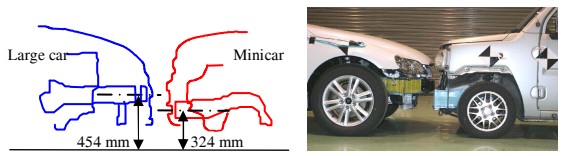

(a) Test 1: Original height

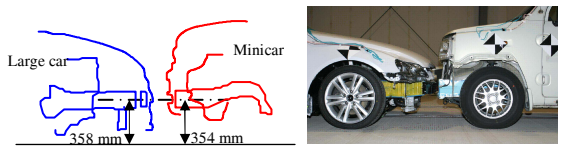

(b) Test 2: Height matching

Figure 10. Structure geometry in Test 1 and Test 2

Test Results

Car Behavior

The car behavior during impact in Tests 1 and 2 is presented in Figure 11. In both tests, the minicar was pushed rearward by the large car. In Test 1, it was observed that the large car overrode the minicar. During the first 20 to 60 ms of the crash sequence, the crash interface moved upward and both cars slid relative to each other. At about 50 ms, the front wheels of the large car separated from the ground and overrode the front wheels of the minicar. Beyond 60 ms of the crash sequence, pitching of the minicar occurred with the rear wheel losing contact with the ground. In Test 2, the structures of both cars interacted and the crash interface did not move in a vertical direction. Pitching of the minicar occurred, whereas the attitude of the large car did not change appreciably.

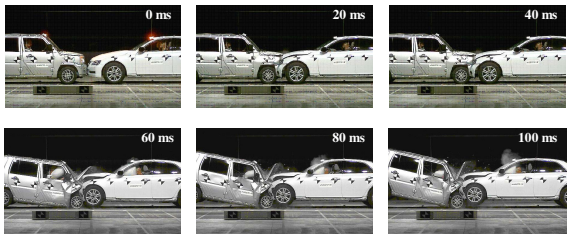

(a) Test 1

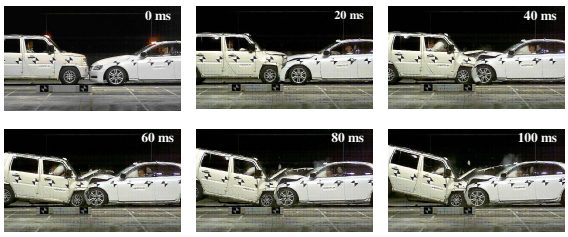

(b) Test 2

Figure 11. Car behavior in car-to-car full frontal tests

Car Deformation

Figure 12 and Figure 13 present deformation patterns of the minicar and large car after the tests. The measured deformations at selected locations are shown in Figure 14. In Test 1, the deformations of front rails of the minicar car were small due to their height mismatch against the large car. For the minicar, the deformation of the right and left front rails was 180 and 153 mm, respectively. The deformation of the upper structures of the minicar was large, and the engine rotated rearward. Additionally, inside the passenger compartment, the intrusion of the instrument panel was 39 mm on the right side and 44 mm on the left side, and the steering column moved rearward by 35 mm and upward by 63 mm. As shown in Figure 5, the steering column rotated upward; and, due to dummy contact, the steering wheel bent and fractured.

In Test 2, the front structures of the minicar deformed uniformly. The car deformation mode was comparable with that in the FRWB test in JNCAP. The deformation of the right and left front rail was 302 and 261 mm, respectively, which was large compared to Test 1. The intrusion of the upper part of the passenger compartment was small. The rearward and upward deformation of the steering column was 12 mm and 33 mm. However, in Test 2, the deformations of the lower structures of the minicar were large, particularly for the transmission bottom (110 mm). As a result of the large deformations, the intrusion of the toe board for the front passenger side was large (143 mm).

(a) Minicar

(b) Large car

Figure 12. Car deformation (Test 1)

(a) Minicar

(b) Large car

Figure 13. Car deformation (Test 2)

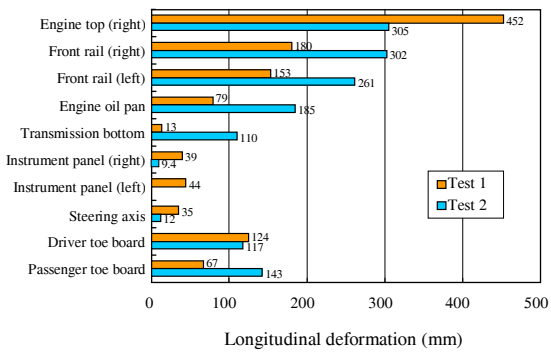

Figure 14. Minicar deformation in Test 1 and 2

Car Acceleration

The accelerations of the passenger compartment are shown in Figure 15. In general, the acceleration pulses are comparable between Test 1 and 2. However, in Test 1 and Test 2, there are differences in the car accelerations at the time of the initial stage of impact. For the first 15 ms, the minicar acceleration was higher in Test 2 because the front rails of both cars made contact with each other. On the other hand, the peak acceleration of the minicar was higher for Test 1 (619 m/s^2) than for Test 2 (539 m/s^2). For the large car, the car acceleration in the initial stage was also high in Test 1 as compared to that in Test 2. The maximum car acceleration was similar in Test 1 (331 m/s^2) and Test 2 (341 m/s^2). Compared to the JNCAP FWRB 55 km/h tests, the time duration was longer for the minicar and shorter for the large car since the minicar is stiffer than the large car.

Injury Measures

According to the video analysis, the driver airbag of the minicar started to deploy at 24 ms, 17 ms, and 14 ms in Test 1, Test 2, and the FWRB test, respectively. Thus, the timing of the airbag deployment was delayed in Test 1 by 7 ms later than that in Test 2. The shoulder belt tension also started late in Test 1 due to the delay of the seat belt pretensioner activation. As a consequence of this delay of the seat belt forces, the acceleration of the head and chest started later by 7 ms in Test 1 compared to Test 2.

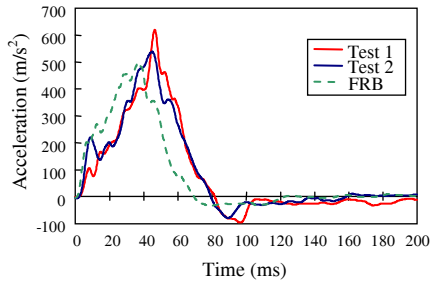

(a) Minicar

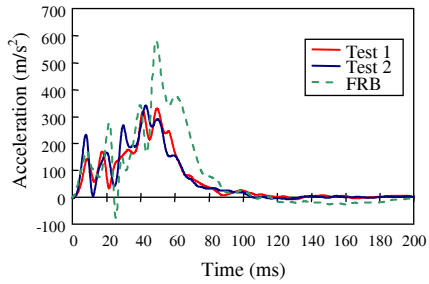

(b) Large car

Figure 15. Car acceleration measured at the B-pillar bottom in car-to-car test and full-width rigid barrier test (JNCAP)

The injury measures of the dummies were compared for Test 1 and Test 2. Figure 16 and Figure 17 show the ratios of the injury measures of the driver and front passenger dummies to the injury assessment reference values (IARVs) of ECE R94, respectively. For the minicar, the injury measures of the driver dummy were larger in Test 1 than those in Test 2. In Test 1, some injury maesures of the driver dummy in the minicar exceeded the IARVs due to the high acceleration and large intrusion of the car. Especially, the neck extension moment, knee displacement (right), and tibia index (right) exceeded their respective IARVs. In Test 2, the head acceleration, neck extension moment, and chest acceleration also exceeded the IARVs, but these measures were less than those in Test 1. As shown in Figure 12 and Figure 13, the steering column of the minicar rotated upward in Test 1 and Test 2. This steering upward rotation was more apparent in Test 1, so that the HIC, chest acceleration, and neck extension moment were large in Test 1. For the front passenger dummy, the injury measures were also larger in Test 1, with the exception of the left tibia axial force and tibia index (see Figure 17). In Test 2, the toe board intrusion of the front passenger of the minicar was large due to large rearward displacement of the transmission. It is likely that this large intrusion led to the large tibia axial force of the front passenger dummy.

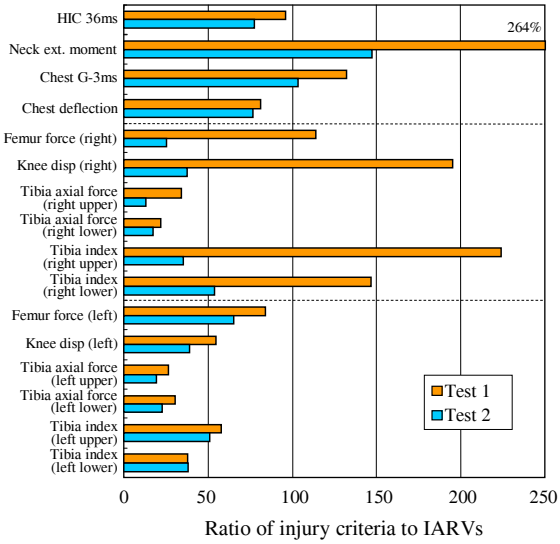

Figure 16. Injury criteria of driver dummy in minicar

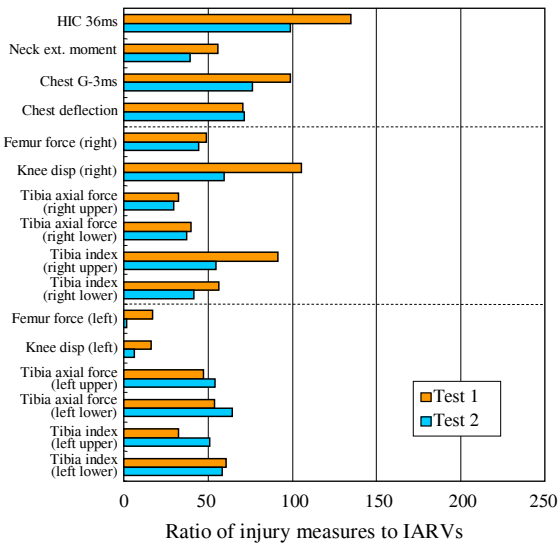

Figure 17. Normalized Injury measures of the front passenger dummy in the minicar

Summary of Crash Test Results

The front rails of the minicar and large car passed by and did not contact each other in Test 1; whereas, they made contact with each other in Test 2. The driver airbag deployment was delayed by 7 ms in Test 1 compared to Test 2 for the minicar. It is likely that the crash sensing at the front rail was affected by the front rail height mismatch. The delayed airbag deployment starting time affected the interaction between the airbag and the dummy head. The height mismatch of the front rails also led to the large intrusion of the upper part of the passenger compartment of the minicar. When the height of front rails were matched (Test 2), the front structure deformed in a comparable mode as observed in the JNCAP FWRB 55 km/h test. As a result, the car acceleration, deformation, and the dummy kinematics in the car-to-car full frontal crash responded in a controlled manner, which was comparable to those in the FWRB tests. These results confirmed that height matching of front rails has advantages in car-to-car collisions in that the car deformation and dummy response could be predicted in a designed mode in crash tests.

The passenger compartment intrusion of the minicar was more severe for Test 1 where the front rail heights were mismatched. In Test 2, where the front rails heights of the two cars matched, the intrusion and the dummy injury criteria could be improved. The matching of front rail height would have the benefit of preventing serious injuries in severe crashes where the intrusion of the passenger compartment is large. However, it should be noted that in crashes at lower velocities, the risk of minor injuries to occupants could be lower when the heights of the car front rails are mismatched. This is because the car acceleration will be smaller when the front rails of the two cars are mismatched in height and they do not generate large crash forces.

CANDIDATE TEST PROCEDURES TO EVALUATE THE FRONT RAIL HEIGHTS

In the WG, four test procedures were proposed to evaluate the front rail heights (Option 1). These tests are based on the evaluation of the barrier force distribution using high resolution load cells (125 mm) in FWRB tests. The FMVSS Part 581 bumper zone is contained within the 3rd and 4th rows of the load cells (Figure 18). As shown in Figure 19, the effect of an engine impact on the force distribution is large in FRWB tests. Accordingly, it is necessary to eliminate the effect of the engine impact in order to evaluate the heights of the structures. If the front rail heights of cars are higher than an established acceptance level, the SEAS should be installed (Option 2). The scope of the test vehicles will be

minicars, ordinary-size cars, and SUVs. In each candidate test, the criteria and acceptance levels are presented below. In some acceptance levels, parentheses [ ] were used to show temporal values.

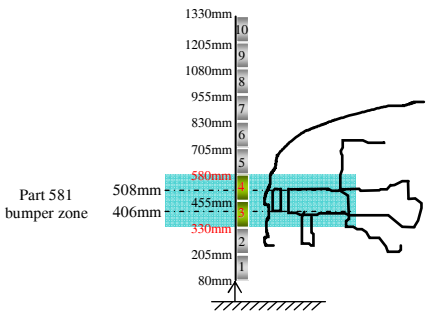

Figure 18. FMVSS Part 581 bumper zone and load cell heights

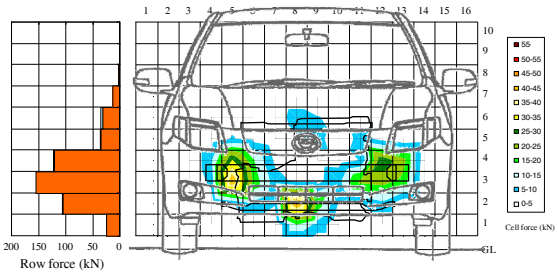

Figure 19. Peak cell force distribution of a small car until car deformation 400 mm in full-width rigid barrier test

Proposed Test 1

In FWRB tests, after the axial collapse of the front rails has commenced, the engine impacts the barrier. Figure 20 plots the barrier force and engine force of cars tested in JNCAP. The engine force is calculated based on the engine mass and acceleration. The engine force is relatively small up to 200 kN of total barrier force. Figure 21 shows the peak cell force distribution of a small car at a total barrier force of 200 kN. The footprint of the front rails is shown clearly. Accordingly, it is likely that the force of these rail structures can be evaluated by analyzing the force distributions up to 200 kN total barrier force.

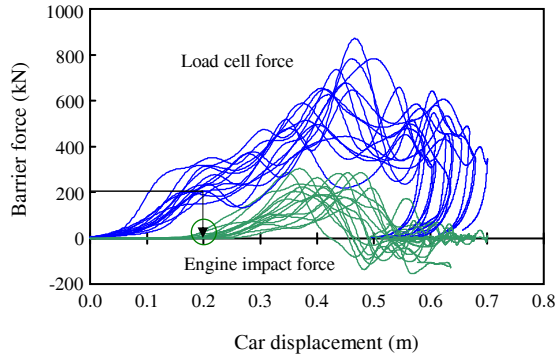

Figure 20. Barrier force and engine impact force in full-width rigid barrier tests (JNCAP 2008)

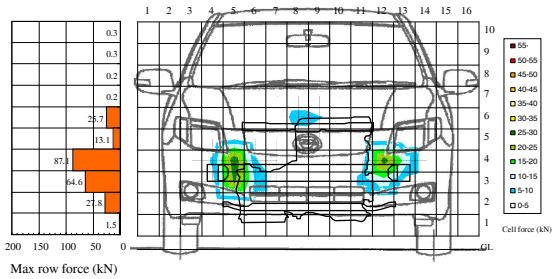

Figure 21. Peak cell force distribution of a small car at total barrier force 200 kN

In a first step, a determination is made whether the front rail height is located between 3rd and 4th row cells. Figure 22 shows the sum of the maximum 3rd and 4th row force at 200 kN total barrier force with the front rail height. The sum of F3+F4 tends to be large as the front rail height is close to the 3rd and 4th row boundary line (455 mm). If the acceptance level of F3+F4 is too high, then the multiple load path cars may not be accepted. Thus, the acceptance level of [80] kN of F3+F4 was used so that only a few cars for which the front rails heights are outside of the 3rd and 4th row are excluded.

In the next step, it is judged that the front rails are located between the 3rd and 4th rows, and whether the front rail cross section includes 455 mm of ground height is examined. Figure 23 shows the relation between the force ratio F4/(F3+F4) and the geometry ratio U/(L+U) (where U is the height between the front rail upper edge and 455 mm, and L is the height between 455 mm and the front rail lower edge). The ratio F4/(F3+F4) is used because the force levels F3 and F4 depend on the front rail stiffness. When 0 < U/(L+U) < 1, the front rail cross

section includes 455 mm height. From Figure 23, the ratio $0 < U/(L+U) < 1$ corresponds to $0.2 < F4/(F3+F4) < 0.8$. The criteria and the acceptance levels of the barrier force for the front rail heights are as follows:

1. F3+F4 > [80] kN
2. [0.2] < F4/(F3+F4) < [0.8]

where F3 and F4 is the 3rd and 4th maximum row force up to the time of 200 kN of total barrier force. If the cars meet the acceptance levels, it is assumed that the cross section of front rail includes the height of 455 mm.

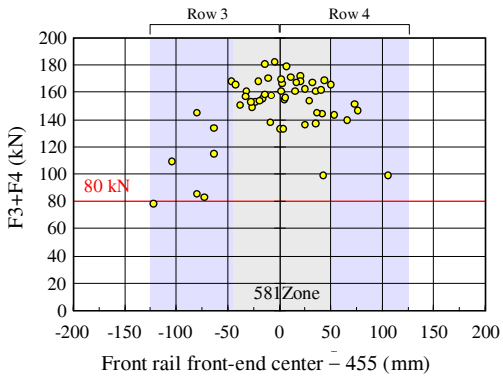

Figure 22. Sum of 3rd and 4th row force and front rail cross section height

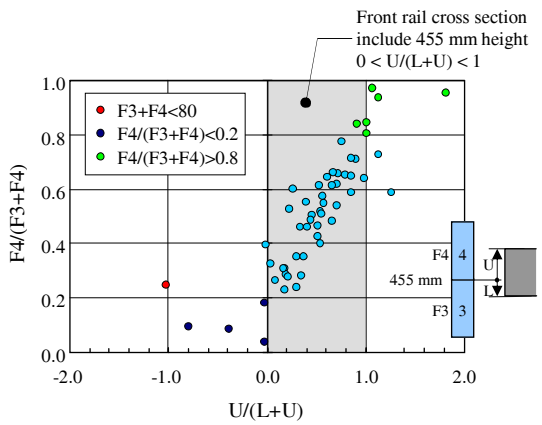

Figure 23. Front rail height and ratio of row force

Figure 24 shows the results of the criteria and the acceptance levels applied to the JNCAP FWRB tests. The cars for which the front rail cross sections do not include 455 mm height were not accepted. It is also shown that the AHOF 400 might not be a good criterion to evaluate the front rail height. The evaluation flow diagram is presented in Figure 25.

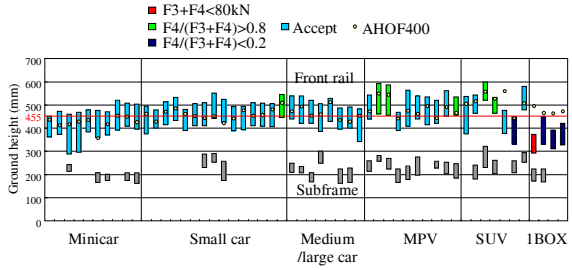

Figure 24. Application of proposed test 1

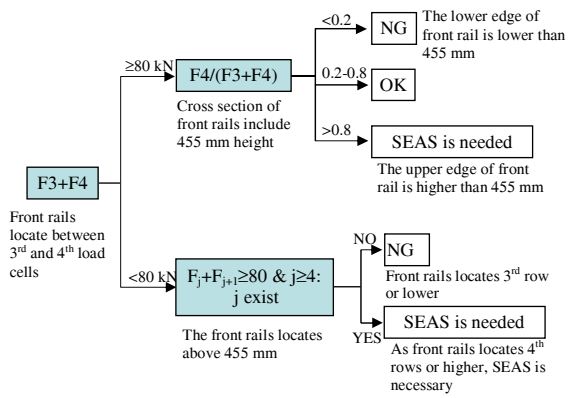

Figure 25. Evaluation flow in proposed test 1

Proposed Test 2

In Option 1, the front rail heights are evaluated. If the cars are not accepted in Option 1, the SEAS will be evaluated in Option 2. The evaluation flow diagram is shown in Figure 26.

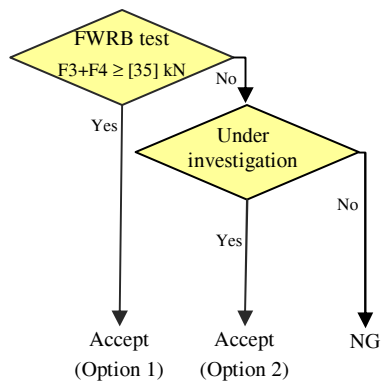

Figure 26. Evaluation flow in proposed test 2

Option 1: The 3rd and 4th row force (F3, F4) in FRWB test are evaluated so that the influence of a SEAS is excluded. The barrier force distributions before the engine impacts the barrier are used to reduce the influence of engine impact force. The criterion is F3+F4, and its acceptance level is [35] kN

as follows (Figure 27):

F3+F4 > [35] kN

where F3 and F4 is the 3rd and 4th maximum row force until 200 kN of total barrier force.

Option 2: Option 2 is dimensional requirement of SEAS, and an evaluation method is under investigation (Figure 28).

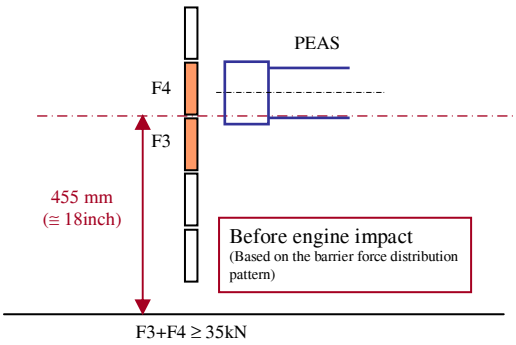

Figure 27. Option 1 test in proposed test 2

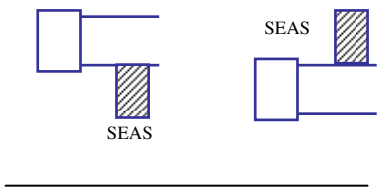

Figure 28. Option 2 test in proposed test 2

Proposed test 3

When a front rail is located in the Part 581 Zone, the force on rows 3 and 4 would be generated mainly by the front-rail stiffness and an engine impact force. Figure 29 shows the (F3+F4)/2 within the center 4 columns until the crush depth 400 mm in JNCAP. Since (F3+F4)/2 in the center 4 columns is less than 100 kN, in general, the engine impact force is less than 100 kN. Accordingly, the car structural force can be evaluated in the 3rd and 4th rows by using the lower limit of 100 kN of (F3+F4)/2.

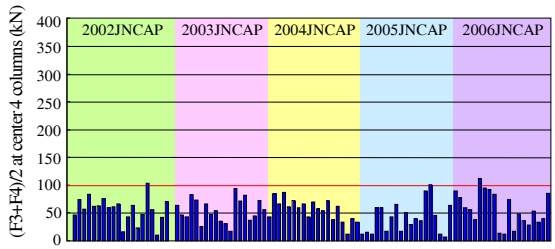

Figure 29. Average of 3rd and 4th rows at center 4 columns in loadcell wall until crush depth 400 mm

In Option 1, the combined force on rows 3 and 4 is evaluated in FWRB test as follows:

(F3+F4)/2 ≥ 100 kN (until 400mm of crush depth)

When the forces generated outside the 3rd and 4th rows are large, the 3rd and 4th row force may not be excited and not be measured correctly. Accordingly, if $(F_n + F_{n+1})/2 \geq (F3 + F4)/2$ (n=4 to 9) until the crush depth 400 mm, an additional test will be carried out to evaluate structural forces that locate at 3rd and 4th rows (Option 2). A evaluation criteria and a flow diagram of the evaluation is presented in Figure 30 and Figure 31.

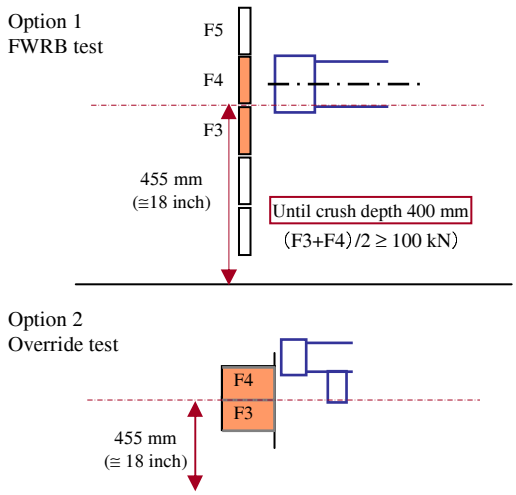

Figure 30. Proposed test 3

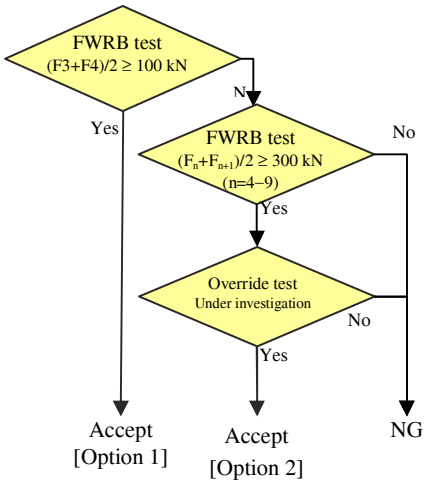

Figure 31. Evaluation flow in proposed test 3

Proposed test 4

Proposed test 4 is similar to proposed test 1 except for the criteria and acceptance levels (Figure 32). In Option 1, the barrier row forces are evaluated in FWRB test as follows:

1. F3+F4 ≥ 100 kN
2. F3 ≥ 40 kN
3. F4 ≥ 40 kN

where F3 and F4 is the 3rd and 4th maximum row force until 200 kN of total barrier force. If the cars do not meet the Option 1, an override test or underride test is carried out to evaluate the SEAS as the Option 2. Figure 33 presents the evaluation flow diagram.

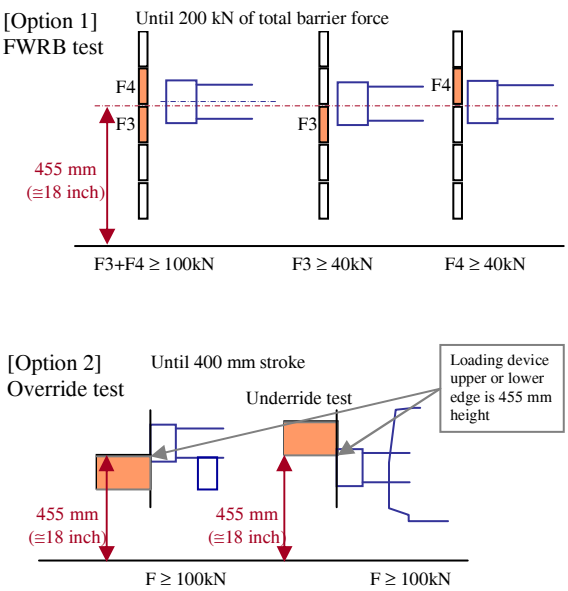

Figure 32. Proposed test 4

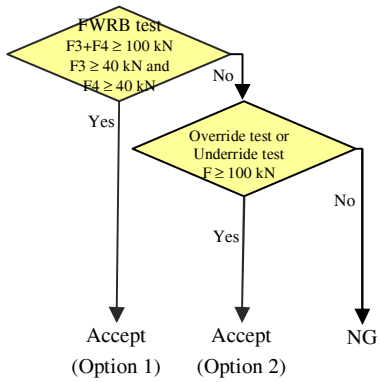

Figure 33. Evaluation flow in proposed test 4

SUMMARY

In the compatibility working group in Japan, the compatibility measures based on the current traffic accident environment in Japan were discussed. The results are summarized as follows.

1. From accident analyses, there is an observed trend that the injury risks increase when the front rail heights are mismatched. However, the front rail heights are related with other factors such as vehicle mass, stiffness, and vehicle class. More research is needed to understand better the effects of front rail height matching.
2. From the full frontal car-to-car crash tests, it was shown that front rail height matching had an advantage of uniform car deformation to prevent large intrusion into the passenger compartment.
3. In the WG, some test procedures to evaluate the front rail heights were proposed that can be used to address one of the identified compatibility problems. In the candidate test procedures, the barrier force distributions were evaluated in full-width rigid barrier tests.

REFERENCES

[1] The Road Transport Subcommittee of Land Transport Committee of Transport Policy Council, "Vehicle Safety Measures for Building a Society Free from Road Traffic Accidents (Report)", 2006.

[2] S Barbat, "Status of enhanced front-to-front vehicle compatibility technical working group research and commitments", Paper number 05-463, 19th international conference on Enhanced Safety of Vehicles, 2005.